Am J Physiol Cell Physiol 309: C81–C91, 2015.
First published May 20, 2015; doi:10.1152/ajpcell.00006.2015.

CALL FOR PAPERS | *Cell Signaling: Proteins, Pathways and Mechanisms*

Thiol-based antioxidants elicit mitochondrial oxidation via respiratory complex III

Vladimir L. Kolossov,[1] Jessica N. Beaudoin,[1] Nagendraprabhu Ponnuraj,[2] Stephen J. DiLiberto,[1] William P. Hanafin,[1] Paul J. A. Kenis,[1,3] and H. Rex Gaskins[1,2,4,5,6]

[1]*Carl R. Woese Institute for Genomic Biology, University of Illinois at Urbana-Champaign, Urbana, Illinois;* [2]*Department of Animal Sciences, University of Illinois at Urbana-Champaign, Urbana, Illinois;* [3]*Department of Chemical and Biomolecular Engineering, University of Illinois at Urbana-Champaign, Urbana, Illinois;* [4]*Department of Pathobiology, University of Illinois at Urbana-Champaign, Urbana, Illinois;* [5]*Division of Nutritional Sciences, University of Illinois at Urbana-Champaign, Urbana, Illinois; and* [6]*University of Illinois Cancer Center, University of Illinois at Urbana-Champaign, Urbana, Illinois*

Submitted 12 January 2015; accepted in final form 13 May 2015

Kolossov VL, Beaudoin JN, Ponnuraj N, DiLiberto SJ, Hanafin WP, Kenis PJ, Gaskins HR. Thiol-based antioxidants elicit mitochondrial oxidation via respiratory complex III. *Am J Physiol Cell Physiol* 309: C81–C91, 2015. First published May 20, 2015; doi:10.1152/ajpcell.00006.2015.—Excessive oxidation is widely accepted as a precursor to deleterious cellular function. On the other hand, an awareness of the role of reductive stress as a similar pathological insult is emerging. Here we report early dynamic changes in compartmentalized glutathione (GSH) redox potentials in living cells in response to exogenously supplied thiol-based antioxidants. Noninvasive monitoring of intracellular thiol-disulfide exchange via a genetically encoded biosensor targeted to cytosol and mitochondria revealed unexpectedly rapid oxidation of the mitochondrial matrix in response to GSH ethyl ester or *N*-acetyl-L-cysteine. Oxidation of the probe occurred within seconds in a concentration-dependent manner and was attenuated with the membrane-permeable ROS scavenger tiron. In contrast, the cytosolic sensor did not respond to similar treatments. Surprisingly, the immediate mitochondrial oxidation was not abrogated by depolarization of mitochondrial membrane potential or inhibition of mitochondrial GSH uptake. After detection of elevated levels of mitochondrial ROS, we systematically inhibited multisubunit protein complexes of the mitochondrial respiratory chain and determined that respiratory complex III is a downstream target of thiol-based compounds. Disabling complex III with myxothiazol completely blocked matrix oxidation induced with GSH ethyl ester or *N*-acetyl-L-cysteine. Our findings provide new evidence of a functional link between exogenous thiol-containing antioxidants and mitochondrial respiration.

antioxidants; glutathione; mitochondria; reductive stress

BECAUSE GLUTATHIONE (GSH) is known to be an integral component of the intracellular antioxidant systems, the cell-permeable pharmacological antioxidant *N*-acetyl-L-cysteine (NAC) is widely used as a supplemental substrate for GSH synthesis. It has been generally assumed that the survival-promoting actions of NAC are due to a direct or an indirect (via intracellular GSH synthesis) action as an antioxidant or as a free radical-scavenging agent (4, 47, 49). Although several reports suggest that NAC protects against oxidation-induced cell death, others claim that NAC also induces apoptosis under certain cellular conditions (14, 31, 39). Increasing evidence challenges the existing dogma that antioxidants such as NAC and GSH can prevent pathological processes solely by ROS detoxification (8, 31, 41). Since antioxidant supplements are widely consumed by many cancer patients during chemotherapy, a more robust knowledge of the mode of action of thiol-containing antioxidants is needed.

Recent studies demonstrate that cellular dysfunction can result from an excessive amount of reducing equivalents in the form of NAD(P)H or GSH in the presence of intact oxidoreductive systems, defined as reductive stress (11, 15, 18–20). Pharmacological and genetic strategies have been used in the most recent studies, which indicate a link between GSH-induced intracellular reductive stress and mitochondrial oxidation and cytotoxicity (50). However, the molecular mechanism for GSH- and NAC-mediated mitochondrial oxidation remains obscure (5, 43, 50).

We hypothesized that mitochondria-specific oxidation was a consequence of increased ROS production in response to reductive stress. This study examines the underlying mechanism of a mitochondria-specific shift toward GSH oxidation in response to the therapeutically relevant antioxidants NAC and GSH. Genetically engineered fluorescent Grx1-roGFP2 redox probes were used for this task. This tool is characterized by improved thiol-disulfide exchange and specificity due to fusion of the roGFP2 probe to the human redox-active enzyme glutaredoxin-1 (Grx1) (16, 32). The cytosol- and mitochondria-targeted probes enabled visualization of previously undetectable early spatiotemporal changes in GSH redox potential (E_{GSH}) in live cells (1, 23, 34).

The data reveal unexpectedly rapid increases in mitochondrial E_{GSH} (to a more oxidizing state) in the mitochondrial matrix after exposure of the cell to NAC or GSH ethyl ester (GEE). However, we questioned how thiol-containing antioxidants might promote immediate intracellular oxidation. By utilizing inhibitors of the multisubunit protein complexes of the mitochondrial respiratory chain, it was possible to identify the origin of antioxidant-induced mitochondrial matrix oxidation. The findings indicate the novel possibility that extracellular thiol-containing antioxidants can activate a signaling path-

Address for reprint requests and other correspondence: V. L. Kolossov, Carl R. Woese Institute for Genomic Biology, Univ. of Illinois at Urbana-Champaign, Urbana, IL 61801 (e-mail: viadimer@illinois.edu).

way(s) that targets respiratory complex (RC) III of the mitochondrial electron transport chain (ETC), which is implicated in ROS production.

EXPERIMENTAL PROCEDURES

Cell culture, transfection, and inhibitors. Chinese hamster ovary (CHO) and human embryonic kidney (HEK293) cells were maintained in Dulbecco's modified Eagle's medium (DMEM); human colorectal carcinoma (HCT116) cells and transformed porcine (PF161-T) fibroblasts were grown in McCoy's 5A medium and DMEM-Ham's F-10 medium, respectively. All media were purchased from the University of Illinois at Urbana-Champaign Cell Media Facility. Cells were cultured and sorted as previously described (24). Transfections were performed with Lipofectamine 2000 following the manufacturer's protocol (Invitrogen). CHO, HEK293, and HCT116 cells were purchased from American Type Culture Collection (Manassas, VA). PF161-T cells were a gift from Dr. Lawrence Schook (University of Illinois at Urbana-Champaign). NAC, reduced GEE, and the mitochondrial respiratory chain inhibitors rotenone, thenoyltrifluoroacetone, myxothiazol, antimycin A, sodium azide, and oligomycin were prepared in accordance with the manufacturers' suggestions. Unless stated otherwise, all chemical reagents were obtained from Sigma (St. Louis, MO).

Genetic constructs. The cytosolic redox-sensitive sensor Grx1-roGFP2 was cloned into pIRES-puro3 as described previously (22). To target the probe to mitochondria, the mitochondrial matrix targeting sequence adenosine triphosphate synthase protein 9, originating from the fungus *Neurospora crassa*, was used (23). roGFP2 in pEGFP-N1 and Grx1-roGFP2 in pQE60 were gifts from Dr. James Remington (University of Oregon), and mitochondrial Grx1-roGFP2 in pLPCX was a gift from Dr. Tobias Dick (Cancer Research Center, Heidelberg, Germany).

Cell imaging. Imaging protocols are discussed in detail elsewhere (22). Briefly, cells expressing cytosolic or mitochondrial Grx1-roGFP2 were seeded in standard culture medium in μ-Slide eight-well ibiTreat microscopy chambers (Ibidi, Munich, Germany). Time-lapse images were collected with a fluorescence-enabled inverted microscope (Axiovert 200 M, Carl Zeiss, Feldbach, Switzerland). Dual-excitation ratio imaging used 395/11- and 494/20-nm excitation cubes, and an emission filter at 527/20 nm was used for both cubes. Exposure times were set at 100–200 ms, and images were taken every 15 or 30 s. Acquired images were processed with Zeiss Axiovision SE64 Rel6.8 software by hand-selection of four to eight individual cells to obtain multiple regions of interest in each time lapse. The means of emission intensities at 527 nm were exported to Excel files and then corrected by background subtraction.

Determination of mitochondrial membrane potential. The change in mitochondrial membrane potential (MMP) was monitored using the cationic dye tetramethylrhodamine ethyl ester (TMRE; Life Technologies, Grand Island, NY). This lipophilic fluorophore enters the cell and accumulates in mitochondria in accordance with the Nernst equation (13, 38). For visualization of alterations in MMP, cells washed with Dulbecco's PBS supplemented with 5% FBS and 10 mM glucose were loaded with TMRE at a final concentration of 50 nM for 10 min at 37°C prior to imaging. Fluorescence emission was recorded using a 546/10-nm excitation, 565-nm dichroic, and 610/60-nm emission filter set. TMRE fluorescence intensity was analyzed concomitantly with the redox-sensitive sensor. To study the role of MMP in response to thiol-containing antioxidants, the pharmacological MMP uncoupler carbonyl cyanide *m*-chlorophenyl hydrazone (CCCP) was used (38).

Modulation of mitochondrial GSH uptake. To study whether cytosol-to-mitochondria GSH translocation affects the mitochondrial response to extracellular thiol antioxidants, the major GSH transporters dicarboxylate (DIC) and 2-oxoglutarate carriers (OGC) were inhibited with butylmalonate (BM) and phenylsuccinate (PS). Both inhibitors were prepared as 0.1 M stock solutions in Dulbecco's PBS adjusted to pH 7.0. Cells were pretreated with 10 mM BM and PS at 37°C in a 5% CO_2 incubator and exposed to 2 mM GEE during imaging.

Determination of reduction potential. The fraction of roGFP2 in the reduced state was calculated from the ratio of reduced to oxidized roGFP2 using equations described elsewhere (16, 23, 29). Changes in GSH reduction potentials were determined from the Nernst equation (23).

Determination of mitochondrial oxidative stress. MitoSOX Red dye was used to assess mitochondrial matrix ROS level (36). Briefly, HCT116 cells seeded in μ-Dishes (Ibidi) were washed with Hanks' buffer and then stained with 5 μM MitoSOX Red for 30 min in a 5% CO_2 incubator at 37°C. Separate cells were coincubated with 4 mM GEE. The cells were washed twice with Hanks' buffer and then examined using a Zeiss LSM710 confocal laser microscope (514-nm excitation). Further image processing and quantification were performed with Zen 2009 software by selection of multiple regions of interest from individual cells. To confirm production of ROS in the mitochondrial matrix, the membrane-permeable ROS scavenger 4,5-dihydroxy-1,3-benzenedisulfonic acid (tiron) was added to the cells 30 min before the challenge with GEE to give a final concentration of 10 mM (37, 45, 46). Fluorescence intensity values were obtained from three different experiments.

Statistical analysis. Data were analyzed by ANOVA and are reported as means ± SD (23). Significant differences between GEE treatment and control to monitor mitochondrial oxidative stress were determined with Tukey's test. Statistical significance was determined at the 0.05 level.

RESULTS

Thiol-based antioxidants induce immediate oxidation of mitochondrial matrix. To study early compartmentalized changes in E_{GSH} in response to extracellular thiol-containing antioxidants, the Grx1-roGFP2 probe was targeted to the cytosol and mitochondrial matrix of CHO and HEK293 cells and tumorigenic HCT116 and PF161-T cells. Sensor expression was verified by fluorescence imaging; the mitochondrial probe exhibits the characteristic tubular shape of the organelle, while in the cytosol, the fluorescence was diffusely distributed (23).

It should be emphasized that roGFP2 is not oxidized by H_2O_2 directly; rather, Grx1 mediates the redox equilibration of roGFP2 with the subcellular GSH redox potential, which is influenced by the GSH-to-GSSG ratio and the total GSH concentration (Fig. 1*A*).

The properties of Grx1-roGFP2 are based on the monothiol mechanism of glutaredoxins in which an increase in oxidation causes formation of a mixed Grx1-GSH disulfide intermediate via specific reaction of the nucleophilic cysteine of Grx1 with GSSG. Consequently, two additional steps in thiol-disulfide exchange result in formation of the internal disulfide bridge in roGFP2, which reciprocally alters two excitation maxima of the probe (17). The molecular mechanism for Grx1-roGFP2 is described in detail elsewhere (32). The relatively reducing midpoint potential for roGFP2 of −280 mV (pH 7.0) defines the quantitative readout of roGFP2 ~40 mV from the midpoint potential (16). Hence, complete oxidation or reduction of the probe, indicative of relative changes in the GSH-to-GSSG ratio, is not equivalent to full oxidation or reduction of the compartmentalized GSH pool.

Recent studies including our own have demonstrated that genetically encoded probes expressed in the cytosol and mitochondrial matrix are substantially reduced in the basal state (Fig. 1*B*) (1, 17, 23, 35). Ratiometric analysis is expressed

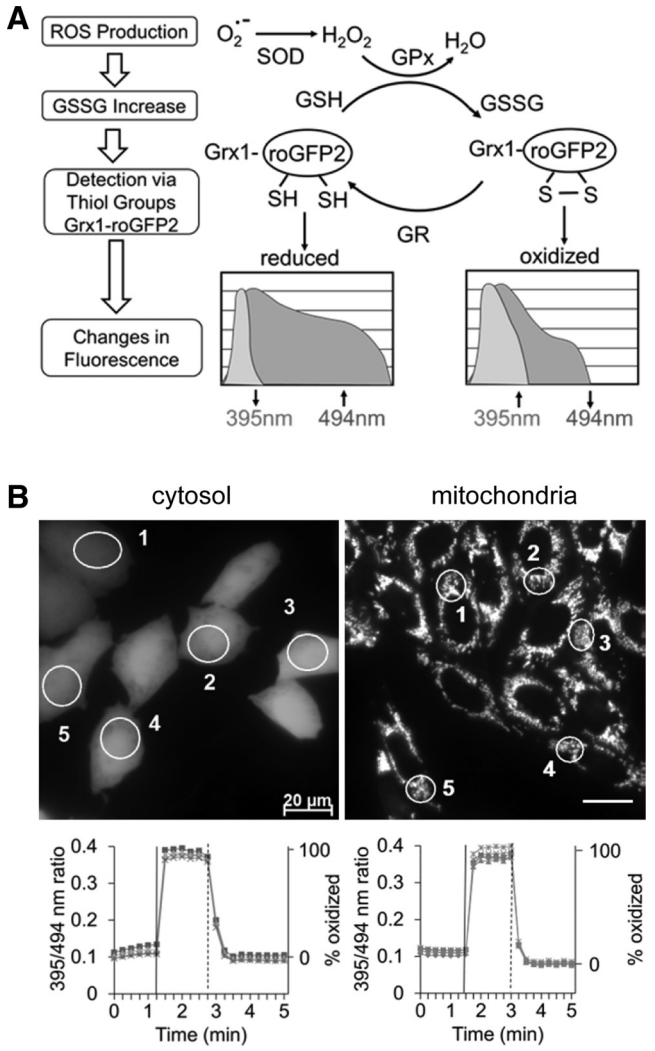

Fig. 1. Schematic of the molecular mechanism of the Grx1-roGFP2 sensor and redox response of the compartmentalized probe to exogenous oxidant and reductant. *A*: $O_2^{\cdot-}$ produced by respiratory complex (RC) III is rapidly converted by superoxide dismutase (SOD) to H_2O_2, which is subsequently reduced by glutathione (GSH) peroxidase(s) (GPx) to water. Glutaredoxin (Grx) fused to roGFP2 efficiently equilibrates the probe with alterations in the GSH-to-GSSG ratio. Thiol-disulfide equilibration is reversible, as GSH reductase (GR) catalyzes reduction of GSSG to GSH. *B*: representative fluorescence images demonstrate the sensor targeted to mitochondrial matrix and cytosol of Chinese hamster ovary (CHO) cells (*top*). *Bottom*: corresponding time-lapse responses of the 395/494-nm ratio to sequential treatment with 2 mM diamide (vertical solid line) to the fully oxidized state and 10 mM DTT (vertical dashed line) to the fully reduced probe state. Each trace designates a separate cell depicted on fluorescence images. Data are representative of 5 independent experiments.

through the time-resolved changes in the excitation ratio of 395- to 494-nm channels (395/494-nm ratio). The 395/494-nm dual-excitation ratio is directly linked to the portion of sensor oxidation: a higher ratio corresponds to stronger oxidative state. The fraction of Grx1-roGFP2 in the oxidized form in the basal state is easily determined with probe calibration through consecutive addition of the oxidant diamide and the reductant DTT to elicit full oxidation (100% oxidation) and reduction (0% oxidation), respectively (Fig. 1*B*).

This process was applied to cells to study intracellular responses to exogenously supplied NAC or GEE. The final concentrations, 4 mM GEE and 5 mM NAC, were chosen to correspond with the expected midpoint of cytosolic and mitochondrial concentrations of GSH in mammalian cells (30). While previous studies with GEE treatments revealed a concentration-dependent trend of toxicity, the effects of ≤4 mM GEE were not significant (48). Representative fluorescence images of cytosolic and mitochondrial probes with corresponding ratiometric analysis are shown in Fig. 2. Under resting conditions, mitochondrial and cytosolic probes are strongly reduced at an excitation ratio slightly above 0.1. After challenge with exogenous GEE, the mitochondrial probe responded with an abrupt transition from a reduced to a fully oxidized state (ratio 0.35) within 30 s. The probe then remained oxidized until DTT challenge rapidly equilibrated the probe to a fully reduced state with an excitation ratio near 0.08, as shown in the GEE time-lapse image in Fig. 2. In contrast, the cytosolic sensor did not respond following GEE application, as shown in GEE time-lapse image. The minor decrease in probe excitation ratio following DTT challenge verified that the cytosolic sensor was almost entirely reduced at the basal state. Therefore, despite the strong mitochondrial response to exogenous GSH, the cytosolic probe is neither oxidized nor further reduced.

To unambiguously confirm immediate compartmentalized responses, we acquired images simultaneously from cytosolic and mitochondrial sensors by coculturing two stably transfected populations of CHO cells in a single well. The fluorescence image of a field populated with both cell lines is depicted in Fig. 2. All visible cells were analyzed, and ratiometric data for two representative cells from each transfected population are shown in the time-lapse images in Fig. 2. Yet again, the probe targeted to the mitochondrial matrix (*cells 1* and *2*) was strongly reduced during resting conditions (first 1.5 min) and rapidly converted to a fully oxidized state within 30 s after GEE application, until subsequent DTT challenge (6 min) resulted in full reduction. In contrast, the probe targeted to cytosol (*cells 3* and *4*) was GEE-insensitive and, as expected, responded in the ratiometric profile shown in Fig. 2.

Cells exposed to NAC responded similarly, as shown in the time-lapse images in Fig. 2. Thus, exogenously supplied thiol-based antioxidants paradoxically trigger mitochondria-specific oxidation, yet they do not affect cytosolic E_{GSH}. Comparable results were observed for multiple cell lines, including tumorigenic HCT116 and PF161-T cells and nontumorigenic HEK293 cells (Fig. 3). To our knowledge, this is the first report of rapid oxidation of the mitochondrial matrix in mammalian cells following exogenously supplemented thiol-containing compounds.

Oxidation of the mitochondrial matrix occurs within seconds and is specific to thiol-based antioxidants. The present data demonstrate that cells respond to challenge with 4 mM GEE by complete saturation of the mitochondrial sensor; after this point, the probe fails to indicate further oxidation. To remain within a suitable range of quantitative sensor readout (±40 mV from its midpoint redox potential), the concentration of GEE was decreased stepwise. Figure 4 shows the mitochondrial probe response expressed in CHO and HCT116 cells after exposure to 2 and 1 mM GEE. Responses to GEE were dose-dependent, rather than time-dependent. The sensor consistently reaches maximum oxidation in seconds and maintains this level in a concentration-dependent manner for several minutes before it equilibrates to the less oxidative state (Fig. 4). The mitochondrial matrix of CHO cells responded to 1 mM

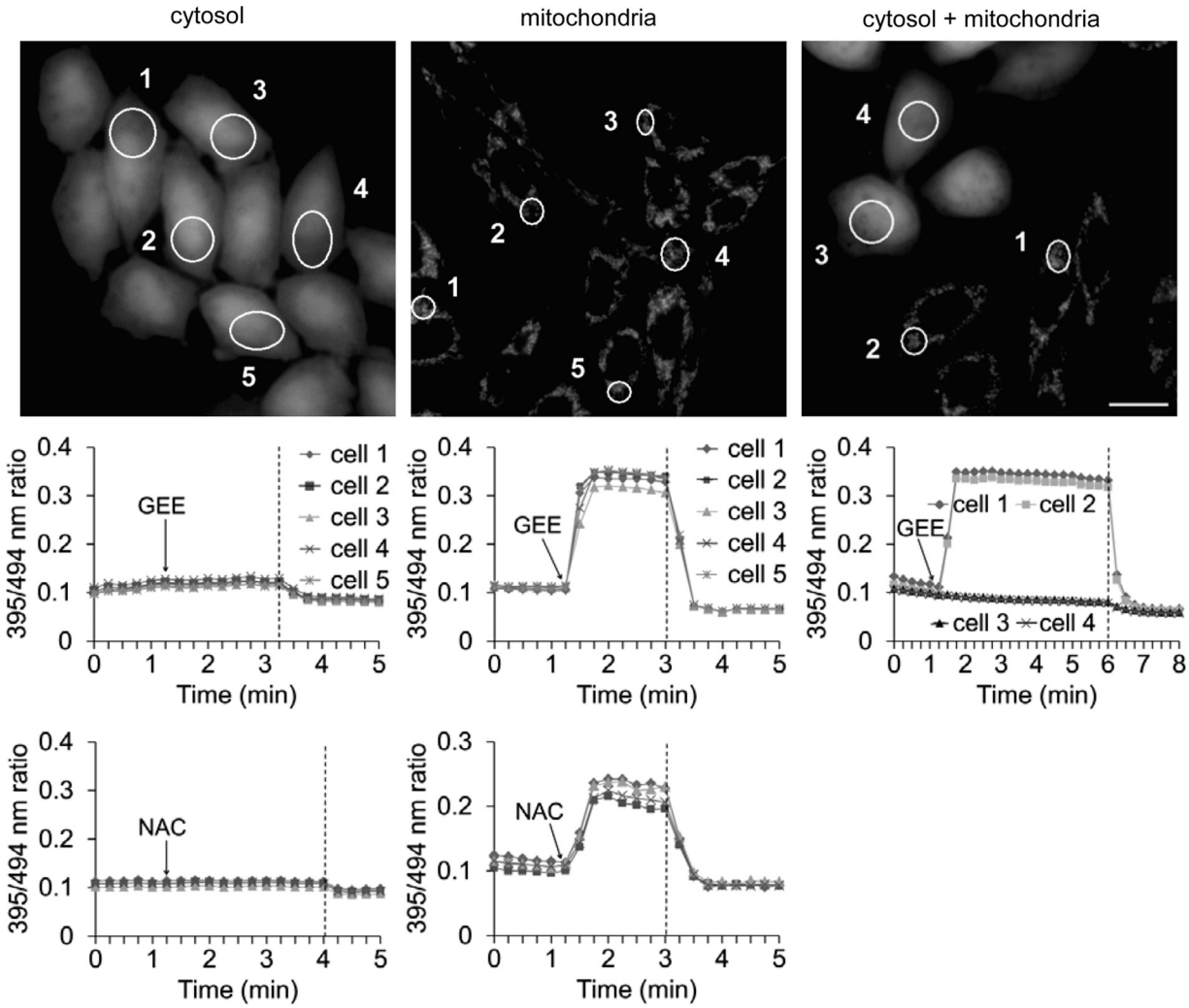

Fig. 2. Differential redox responses of mitochondrial matrix and cytosol to challenge with GSH ethyl ester (GEE) or *N*-acetyl-L-cysteine (NAC). *Top*: representative fluorescence images (494 nm) of the Grx1-roGFP2 sensor targeted to mitochondria or cytosol of CHO cells. Scale bar = 20 μm. *Bottom*: corresponding time-lapse responses of the 395/494-nm excitation ratio to sequential treatment with 4 mM GEE (arrows) or 5 mM NAC (arrows), followed by 10 mM DTT (vertical dashed line). Each trace designates a separate cell depicted on fluorescence images (GEE-treated cells). Data are representative of 5 independent experiments.

GEE with a temporal change of E_{GSH} near 40 mV. Extended time-lapse imaging revealed the transient nature of mitochondrial oxidation (Fig. 4); at 30 min following exposure to GEE, the probe remained in an oxidative state that was slightly higher than baseline (not shown).

We then asked if rapid oxidation of the mitochondrial matrix mediated by thiol-based pharmacological compounds is a specific feature of NAC and GEE and if other endogenously available non-thiol-based antioxidants could trigger similar responses. We utilized ascorbic acid (AA), an integral contributor to thiol homeostasis (42). However, in contrast to NAC and GEE, the mitochondrial probe was insensitive to challenge with AA (Fig. 5*A*). The data show that only thiol-containing compounds trigger mitochondrial oxidation, implying the direct reactivity of sulfhydryl groups.

Rapid thiol-based responses are independent of mitochondrial GSH uptake, biosynthesis, and products of antioxidant hydrolysis. As the various subcellular pools of GSH originate from cytosolic synthesis, it has been generally accepted that GSH accrues in the mitochondrial matrix via uptake through two major putative transporters in the mitochondrial inner membrane, DIC and OGC (26). To determine the contribution of mitochondrial transport to GEE response, we altered GSH uptake with BM and PS, the respective inhibitors of DIC and OGC (10, 26). However, neither of the inhibitors affected the probe response to GEE, even at a reduced concentration of 1 mM (Fig. 6*A*). These data indicate that DIC and OGC are highly unlikely to be involved in the oxidative mitochondrial GEE response, although other GSH transport systems cannot be excluded (7, 26).

After intracellular uptake, esterified GSH and acetylated cysteine are hydrolyzed in the cytosol and exert their antioxidant property. The main protective action of deacetylated NAC is generally attributed to its ability to serve as a precursor to cytosol-synthesized GSH in antioxidant-depleted cells. Hence, the next question was whether NAC deacetylated to cysteine contributes to mitochondrial oxidation directly or via GSH synthesis. As a result, GSH synthesis was inhibited with the

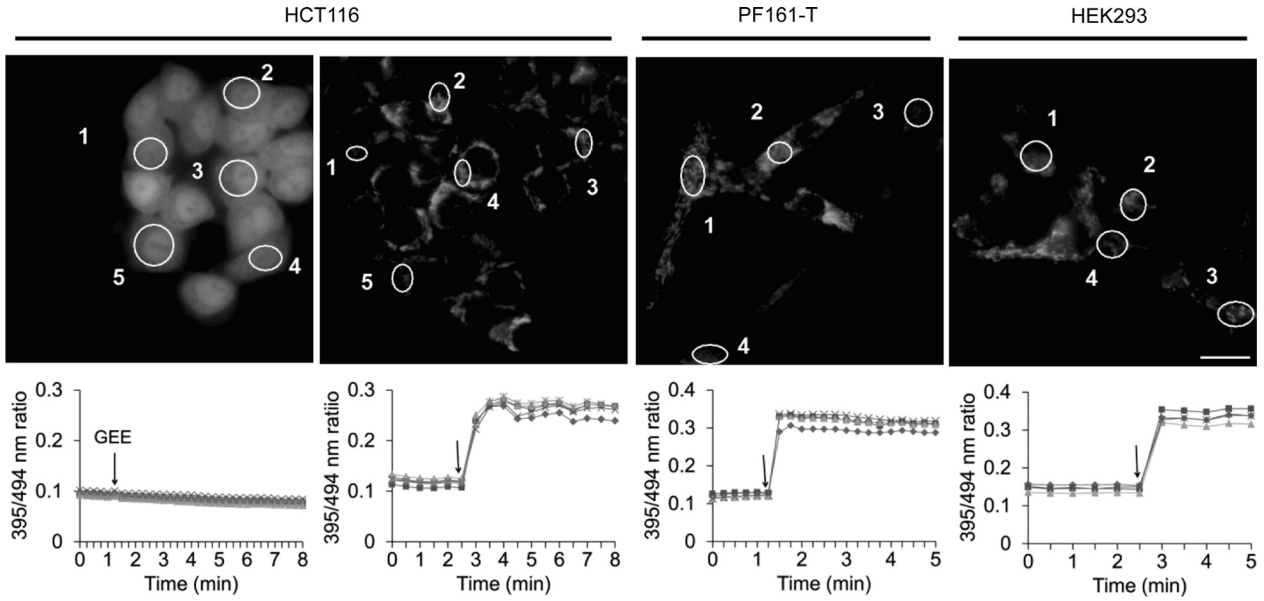

Fig. 3. Differential redox response of mitochondrial matrix and cytosol of various cells to challenge with GEE. *Top*: representative fluorescence (494 nm) images of the Grx1-roGFP2 sensor targeted to cytosol of HCT116 cells and mitochondria of HCT116, PF161-T, and HEK293 cells. Scale bar = 20 μm. *Bottom*: corresponding time-lapse responses of the 395/494-nm excitation ratio to challenge with 4 mM GEE (arrow). Each trace designates a separate cell depicted on fluorescence images. Data are representative of 3 independent experiments.

glutamate-cysteine ligase inhibitor L- buthionine sulfoximine (BSO) before NAC challenge. Figure 6*B* shows similar NAC-induced oxidation of the mitochondrial probe in control and BSO-treated cells. The NAC-mediated change in the probe ratio ranged from 0.1 in the basal state to 0.2 with or without BSO. This result indicates that the mitochondrial response to NAC is independent of GSH synthesis, once again underscoring the active role of exogenous sulfhydryl groups, rather than intracellular GSH content.

Next, as previous studies suggested that toxicity of GEE could be attributed to ethanol, a by-product of GEE deesterification, the extent to which ethanol affected the sensor equilibrium with mitochondrial E_{GSH} was examined (9, 48). In contrast to the GEE response, cytosolic and mitochondrial

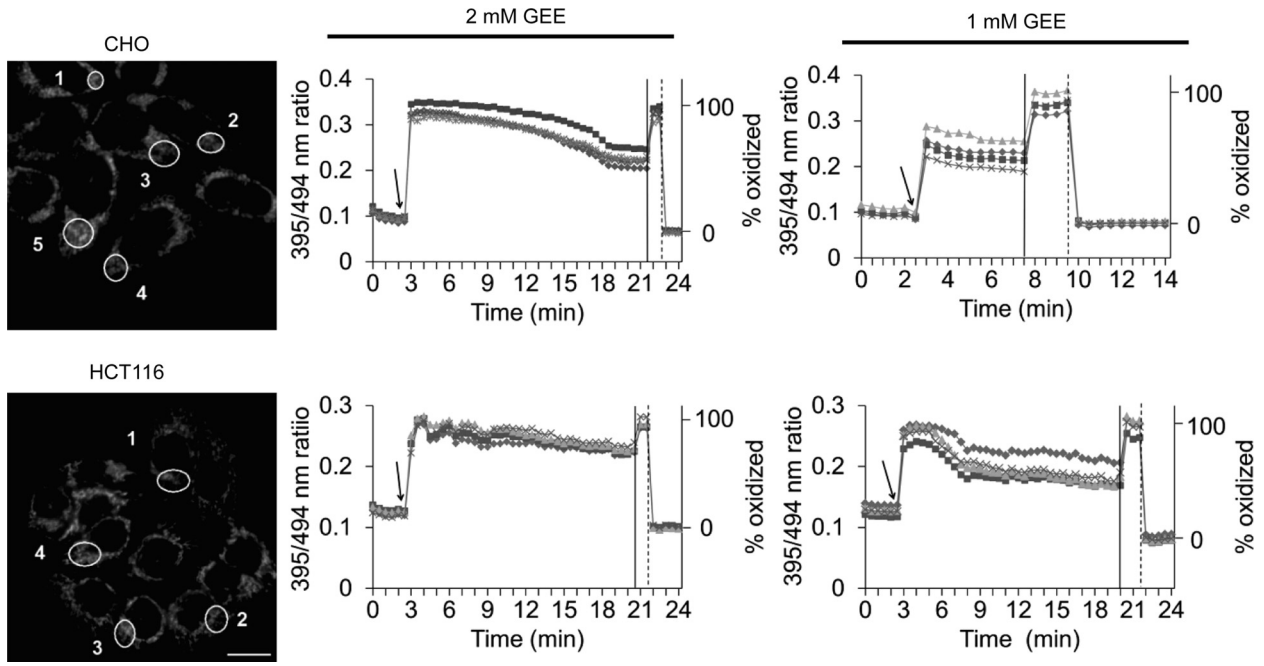

Fig. 4. GEE response triggers immediate transient matrix oxidation in a dose-dependent manner. *Left*: representative fluorescence (494 nm) images of the Grx1-roGFP2 sensor targeted to mitochondria of CHO and HCT116 cells. Scale bar = 20 μm. *Right*: corresponding time-lapse responses of the 395/494-nm excitation ratio to sequential treatment with 2 and 1 mM GEE (arrow), 2 mM diamide (vertical solid line), and 10 mM DTT (vertical dashed line). Each trace designates a separate cell. Data are representative of 3 independent experiments.

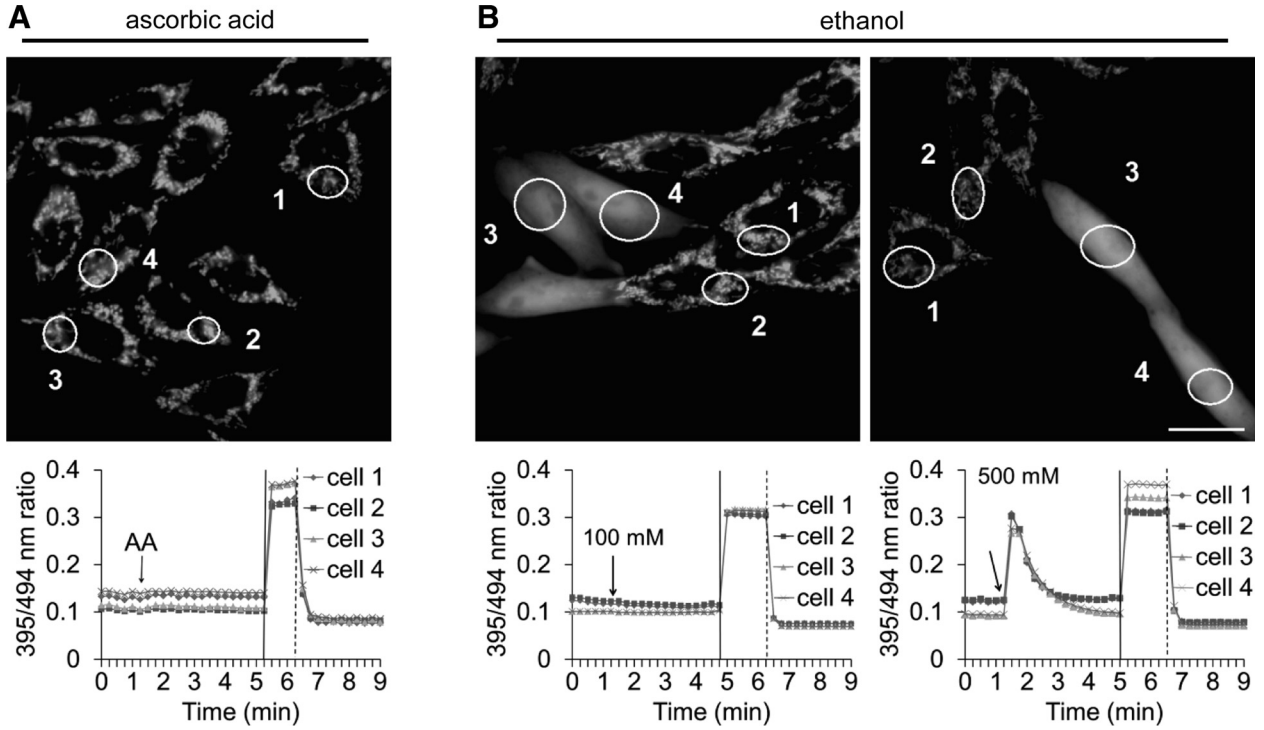

Fig. 5. Effects of ascorbic acid (AA) and ethanol on the mitochondrial probe response. *Top*: fluorescence images show CHO cells expressing mitochondrial Grx1-roGFP2 exposed to 5 mM AA (*A*) or 100 or 500 mM ethanol (*B*) at 1.5 min. Scale bar = 20 μm. *Bottom*: time-lapse responses of the 395/494-nm excitation ratio corresponding to fluorescence images. For the probe, calibration cells were treated with 2 mM diamide (solid line) and 10 mM DTT (dashed line). Scale bar = 20 μm. Each trace designates a separate cell depicted on the images. Data are representative of 3 independent experiments.

probes responded similarly in a concentration-related manner: oxidation with 500 mM ethanol was followed by immediate probe recovery to the basal state in both compartments (Fig. 5*B*). Although this concentration caused considerable oxidation, early production of intracellular ethanol resulting from deesterification of membrane-permeable GEE is considerably lower (28, 48). Thus, while alcohol at high concentrations also rapidly perturbs mitochondrial redox homeostasis, an ethanol effect on GEE response is highly unlikely due to the concomitant oxidation of the cytosol, in contrast to thiol antioxidants.

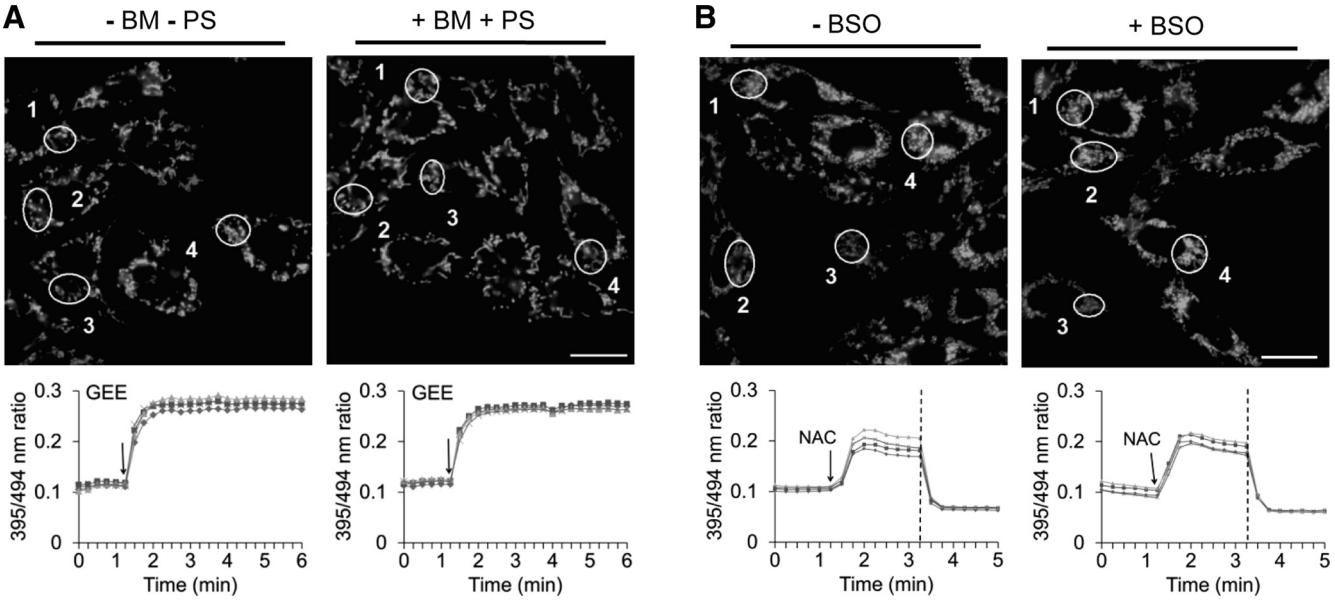

Fig. 6. Thiol-based responses are independent of GSH uptake and synthesis. *Top*: fluorescence images show CHO cells expressing mitochondrial Grx1-roGFP2 challenged with 1 mM GEE following pretreatment with or without butylmalonate (BM) and phenysuccinate (PS) for 2 h (*A*) or 5 mM NAC following pretreatment with or without buthionine sulfoximine (BSO) for 30 min (*B*). Scale bar = 20 μm. *Bottom*: corresponding time-lapse responses of the 395/494-nm excitation ratio to GEE (arrow) or sequential treatment with NAC (arrow) and DTT (dashed line) at 10 mM. Each trace designates a separate cell depicted on fluorescence images. Data are representative of 3 independent experiments.

GEE response does not require an intact mitochondrial respiratory chain. A strong correlation exists between ROS production and MMP, which characterizes mitochondrial fitness (44). To further elucidate the mechanism of mitochondrial matrix oxidation with extracellular thiol-containing compounds, we followed MMP responses via live cell imaging. Cells were loaded with the well-documented fluorescent dye TMRE, and alterations in membrane potential and the mitochondrial probe E_{GSH} were simultaneously measured initially in the basal state for 2 min and then in response to GEE. Surprisingly, in contrast to rapid sensor oxidation, no immediate change in fluorescence intensity of TMRE dye was observed following GEE application, as shown in Fig. 7*A* for two representative cells. Images in Fig. 7*A* illustrate alterations in probe and TMRE fluorescence during transition from the basal state and following subsequent challenge with GEE at 1 and 5 min. The decrease in probe fluorescence intensity at 494 nm (green) corresponds to higher mitochondrial oxidation, while no change in TMRE (red) fluorescence indicates stable MMP. Cells lacking probe expression can be visualized only by TMRE staining.

Because GEE does not immediately alter MMP, we next asked if the GEE response is modulated by MMP. Since MMP generated by the flux of electrons via the mitochondrial ETC has been associated with ROS production, the uncoupler CCCP was used to dissipate the MMP. Figure 7*B* shows that depolarization of MMP, indicated by a decrease in TMRE fluorescence, occurred within minutes following challenge with CCCP. Time-resolved probe responses were concurrently monitored. Loss of MMP with CCCP treatment failed to considerably alter the 395/494-nm ratio in the probe at the basal state and to affect GEE-induced probe oxidation (Fig. 7*B*). Time-lapse images illustrate changes in fluorescence intensity of the mitochondrial Grx1-roGFP2 probe and TMRE dye before and after treatments. Together, these results imply a GEE response independent of MMP under our experimental conditions.

GEE triggers mitochondrial ROS production. To test our hypothesis that the thiol-mediated increase in ROS formation contributes to oxidation of the mitochondrial matrix, the mitochondrial ROS-specific dye MitoSOX Red was used. Figure 7*C* shows GEE-induced oxidation of the probe with a 50% increase in fluorescence intensity. Representative fluorescence images show a visible increase in dye fluorescence intensity. Consequently, we evaluated the membrane-permeable compound tiron, which exhibits antioxidant effects as a metal chelator and a radical scavenger, to determine whether ROS neutralization would reverse the oxidation caused by GEE (37, 46). HCT116 cells were exposed to 10 mM tiron for 30 min and then to 1 mM GEE. Indeed, tiron abrogated the response to GEE within 1 min (Fig. 7*D*) compared with tiron-free cells (Fig. 4). Rapid sensor oxidation in the presence of tiron presumably indicates superior kinetics of the sensor response to GEE-induced ROS generation compared with the scavenging kinetics of tiron. These data represent the first direct observation of a rise in mitochondrial ROS activity following application of exogenous thiol-containing antioxidants and may indicate that ROS generated from mitochondrial sites are responsible for oxidation of the probe.

Thiol-based antioxidants elicit spatial oxidation via mitochondrial RC III. The next crucial step in validation of the hypothesis of a ROS-mediated response to extracellular thiols was identification of the specific mitochondrial site(s) generating ROS. Mitochondria are the major source of intracellular ROS formation, 90% of which is ascribed to the ETC. Mitochondrial respiration is affected in many pathological conditions, and impaired ETC performance could emit additional ROS. To examine whether extracellular thiol-induced ROS production is linked to mitochondrial respiration, well-established inhibitors of RCs were utilized in concentrations necessary to completely block respiration in tumorigenic HCT116 or normal CHO cells (21). Figure 8*A* shows the response of each RC and ATPase of HCT116 cells to corresponding inhibitors, which were individually applied 3 min prior to GEE challenge. Inhibition of RC I, RC II, RC IV, and ATPase did not prevent immediate oxidation in response to 2 mM GEE. In contrast, antimycin A profoundly diminished, and myxothiazol fully abolished, the probe response to GEE in HCT116 (Fig. 8*A*) and CHO (data not shown) cells. At high concentrations, antimycin A fully oxidized the sensor and, therefore, diminished its utility for further study. Consequently, the antimycin A concentration was decreased to 1 μM, resulting in a complete lack of sensor response or mild oxidation with rapid recovery. Whereas this concentration is presumably sufficient to inhibit RC III, the detection of antimycin-induced ROS production in cell culture is indeed time- and concentration-dependent (36). The observation that inhibition of RC III prevents the mitochondrial sensor oxidation implies that semiquinone formation in the Q cycle is responsible for $O_2^{\cdot -}$ production. Myxothiazol, which demonstrated the most pronounced effect, was chosen for further experiments. Taken together, our data on independence of the GEE response from the inhibition of other respiratory chain complexes are in agreement with the absence of MMP alterations and, therefore, provide additional evidence that RC III, but not an intact mitochondrial respiratory chain, is required for ROS production.

Thiol-induced mitochondrial oxidation is rescued by inhibitors of RC III. Because brief pretreatment of cells with myxothiazol blunted NAC- and GEE-mediated responses, we asked whether RC III inhibition could rescue the probe already oxidized by thiol-based antioxidants. Figure 8*B* shows successive cell treatment with GEE, myxothiazol, and DTT. Remarkably, myxothiazol fully restored the oxidized probe to the basal reduced state within minutes. A similar result was observed for the probe oxidized with NAC (data not shown). More importantly, this outcome refutes the possibility of an acidification-induced probe oxidation via acetic acid, a by-product of NAC deacetylation by cytosolic esterases. These data clearly demonstrate that RC III is a major site of ROS production following exogenous thiol-containing antioxidant treatment.

DISCUSSION

Previous evidence suggests that exogenously supplied NAC triggers gradually induced oxidation of mitochondrial matrix E_{GSH}, despite decreased levels of ROS (50). Because the precise mechanism of mitochondrial oxidation without ROS elevation is unknown, we further examined the early response of compartmentalized E_{GSH} to NAC and GEE applications via time-resolved imaging. We hypothesized that excessive gener-

ation of mitochondrial ROS precedes the rapid shift of E_{GSH} toward oxidation.

Here, mitochondrial ROS production, as revealed by MitoSOX Red, is consistent with previous reports of increased ROS concentrations in NAC-treated mouse embryonic fibroblasts (31), rat myoblasts (43), human androgen-independent prostate cancer cells (27), and pancreatic cancer cells (33). In fact, studies on mouse fibroblasts suggested two modes of action for NAC: *1*) immediate, when NAC acts as prooxidant within 1 h, and *2*) as a thiol antioxidant at around 24 h and

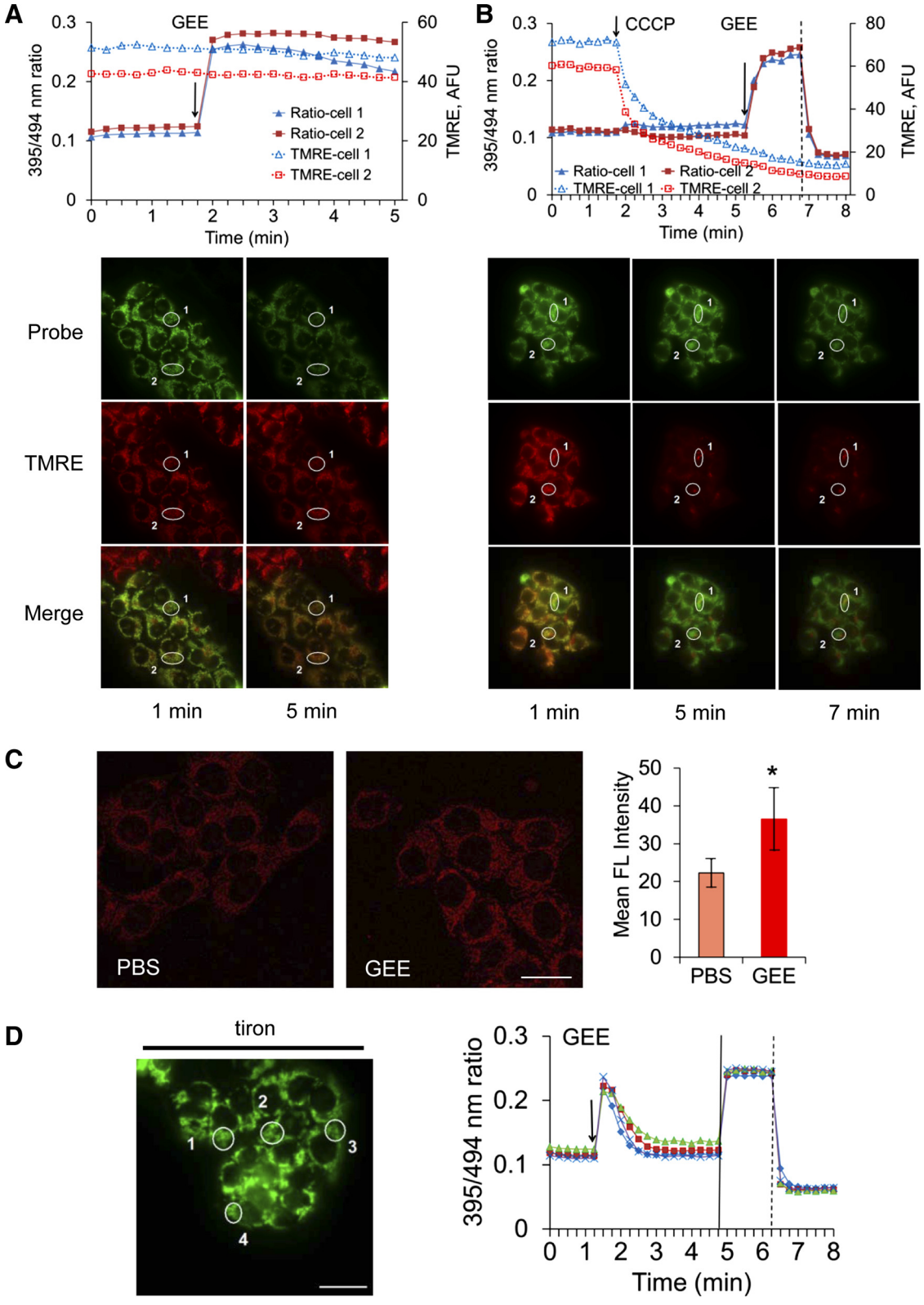

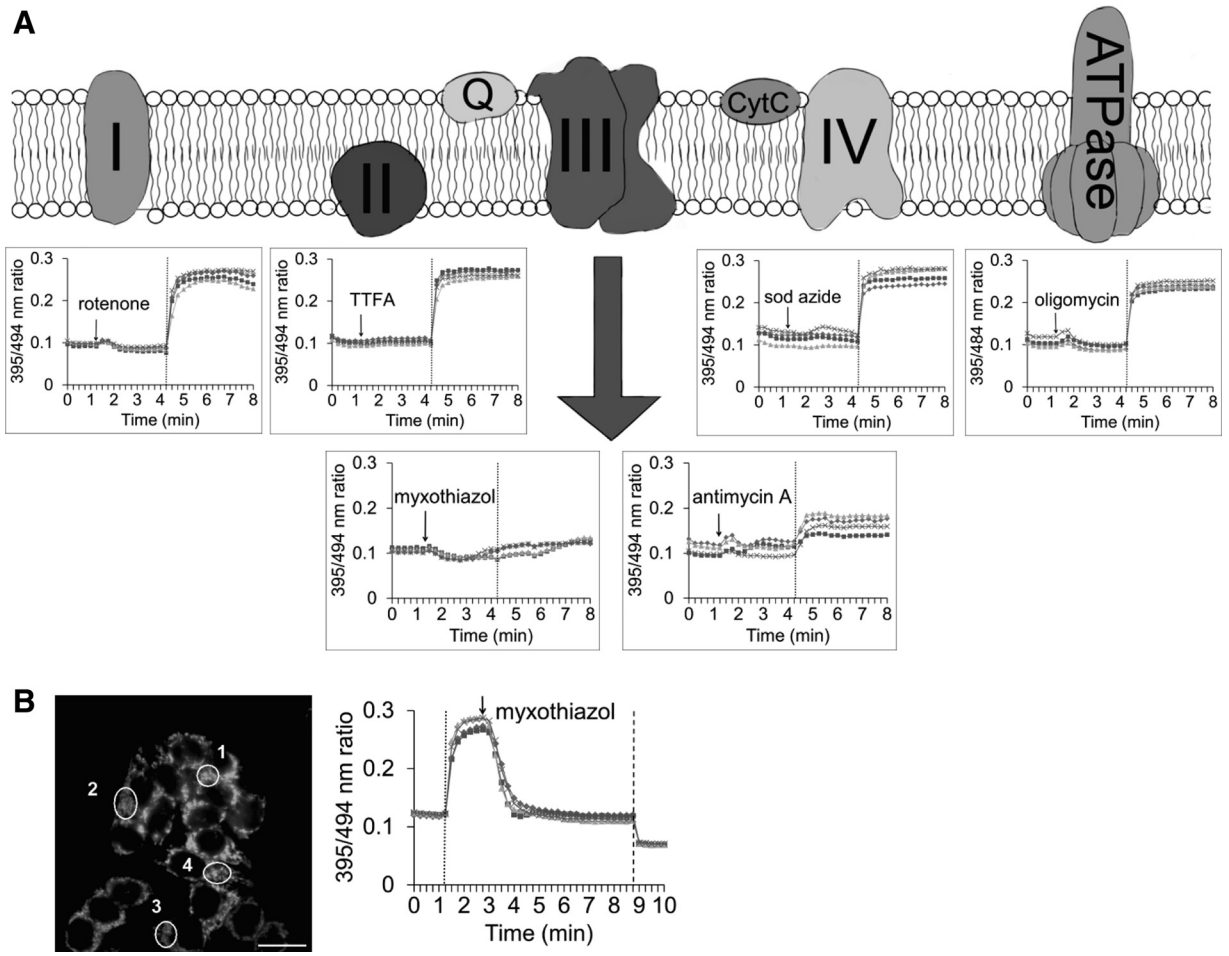

Fig. 8. Extracellular thiol-containing antioxidants target mitochondrial RC III. *A*: schematic of mitochondrial respiratory chain with representative time-lapse responses of 395/494-nm ratio of the mitochondrial Grx1-roGFP probe targeted to HCT116 cells with exposure to 1 μM rotenone, 100 μM thenoyltrifluoroacetone (TTFA), 1 μM antimycin A, 1 μM myxothiazol, 0.5 mM sodium azide, or 10 μM oligomycin (arrows at 1.5 min) to sequential treatment of 2 mM GEE (dotted vertical line). Only inhibition of RC III altered the probe response to GEE. Q, Q cycle; CytC, cytochrome *c*. *B*: representative fluorescence (494 nm) image of the Grx1-roGFP2 sensor targeted to mitochondria of HCT116 cells (*left*). *Right*: time-resolved responses of the probe to sequential treatments with 2 mM GEE (solid line), 1 μM myxothiazol, and 10 mM DTT (dashed line). Each trace designates a separate cell depicted on fluorescence images. Data are representative of 3 independent experiments. Scale bar = 20 μm.

beyond (31). However, the mechanisms generating NAC-induced ROS were not investigated (2, 31, 33). While intracellular ROS production is generally measured after hours of exposure to compounds of interest, our data indicate immediate release, as evidenced by the ability of the membrane-permeable ROS scavenger tiron to attenuate rapid mitochondrial probe oxidation.

We further hypothesized that the ROS-generating site was contained within the mitochondrion. To locate the origin of thiol-mediated ROS production, we applied mitochondrial respiratory chain inhibitors during live cell imaging. This approach revealed RC III as a novel downstream target of thiol antioxidants. Inhibition of RC III with antimycin A significantly diminished the oxidative response to thiol-based anti-

Fig. 7. Independent of mitochondrial membrane potential (MMP), GEE response leads to ROS formation. *A* and *B*: HCT116 cells transfected with mitochondrial probe and loaded with tetramethylrhodamine ethyl ester (TMRE) dye for MMP visualization were challenged with 2 mM GEE or successively with 5 μM carbonyl cyanide *m*-chlorophenyl hydrazone (CCCP), 2 mM GEE (arrows), and 10 mM DTT (dashed line). *Top*: changes in sensor excitation ratio and fluorescence intensity of TMRE dye over time for 2 representative cells. *Bottom*: fluorescence emission (494- and 546-nm double-excitation) micrographs show changes in GSH redox potential (E_{GSH}) via the mitochondrial Grx1-roGFP2 sensor (green) and MMP with TMRE dye (red) at indicated time points. Decrease in probe fluorescence intensity at 494 nm (green) corresponds to higher mitochondrial oxidation, while decrease in TMRE (red) fluorescence indicates loss of MMP. *C*: representative confocal images of HCT116 cells (514 nm) showing increase in mitochondrial MitoSOX Red fluorescence following treatment with 4 mM GEE for 30 min (*left*). *Right*: relative fluorescence intensity for MitoSOX Red staining of GEE-treated or untreated (PBS) HCT116 cells. *D*: fluorescence micrograph (494 nm) of the mitochondrial probe expressed in HCT116 cells exposed to 10 mM tiron for 30 min (*left*). *Right*: corresponding time-lapse responses of the 395/494-nm ratio to sequential treatment with 1 μM GEE (arrow), 2 mM diamide (vertical solid line), and 10 mM DTT (vertical dashed line). Each trace designates a separate cell depicted on the images. Values are means ± SD, $n = 3$. Scale bar = 20 μm. *$P < 0.01$ vs. non-GEE-treated cells. Data are representative of 3 independent experiments.

oxidants, while myxothiazol demonstrated the most pronounced neutralizing effect. Furthermore, myxothiazol fully rescued the mitochondrial probe following oxidation with exogenous thiols. These findings indicate a functional link between mitochondrial respiration and environmental thiol-induced stress through a contributing role of RC III in ROS release, which results in more oxidizing E_{GSH} of the mitochondrial matrix.

Simultaneous time-lapse imaging of the probe and fluorescent TMRE dye used for assessment of MMP did not reveal MMP alteration, despite rapid oxidation of the probe in GEE-exposed HCT116 cells. Whereas the probe oxidation is in agreement with $O_2^{\cdot -}$ production by RC III, the apparent discrepancy rests in a dissonance between ROS production and the absence of MMP alterations. However, it should be emphasized that this result is consistent with the recent observation that $O_2^{\cdot -}$ production by RC III does not depend on mitochondrial transmembrane potential (12, 25). It should also be noted that immediate oxidation of the probe with 2 mM GEE indicates oxidation of ~2% of the mitochondrial GSH pool, an alteration presumably too insignificant to impair MMP, which is in line with recent results suggesting that some compounds generate $O_2^{\cdot -}$ at concentrations lower than necessary to impair MMP (6). Our data are consistent with previous findings that ≤15 mM NAC did not induce alterations in MMP in pancreatic cancer AsPC-1 cells (33). While Grx1-roGFP2 targeted to mitochondria of HeLa cells treated with the apoptosis inducer TNF-related apoptosis-inducing ligand (TRAIL) indicated that oxidation of the mitochondrial GSH pool is directly coupled to MMP collapse, this observation is true under the extreme cellular conditions during induced apoptosis on a time scale of several hours, when visual changes in cell shape are clearly pronounced, conditions dissimilar to extracellular thiol treatments (16). Together, these data indicate that cell type and duration, severity, and concentrations of stimuli will determine whether changes in ROS production reflect alteration of MMP.

Although our results offer a new explanation of the origin of extracellular thiol-induced oxidation, it is unclear how relatively small dynamic changes in intracellular thiol content trigger rapid mitochondria-specific ROS production via RC III. The rates of intracellular GEE or NAC uptake are not rapid enough to significantly alter baseline 1–10 mM concentrations of intracellular GSH within seconds (28, 40). The independence of NAC-induced mitochondrial oxidation from GSH synthesis and the inability of AA to trigger mitochondrial oxidation in a similar manner indicate the direct reactivity of their sulfhydryl groups. Furthermore, responses to NAC and GEE are independent of mitochondrial GSH uptake, indicating that these thiol-containing antioxidants do not exert an oxidative effect through accumulation and subsequent reduction of the electron carrier pools leading to ROS release, as suggested by the reductive stress model (3). In contrast to our initial hypothesis that accumulation of excessive intramitochondrial reducing equivalents in the form of GSH triggers a mitochondria-specific response, we propose that mitochondrial oxidation is possibly mediated by activation of a cellular plasma membrane component(s). Nevertheless, extracellular thiols initiate an unknown cascade that, via reduction of the RC III, may affect cellular energy.

ACKNOWLEDGMENTS

We thank Dr. Shiv Sivaguru and Dr. John Eichorst (Carl R. Woese Institute for Genomic Biology) and Dr. Barbara Pilas (Roy J. Carver Biotechnology Center Flow Cytometry Facility) for their assistance.

GRANTS

This work was supported by National Institutes of Health Grant R33-CA-137719 (H. R. Gaskins and P. J. A. Kenis).

DISCLOSURES

No conflicts of interest, financial or otherwise, are declared by the authors.

AUTHOR CONTRIBUTIONS

V.L.K., P.J.A.K., and H.R.G. developed the concept and designed the research; V.L.K., J.N.B., N.P., S.J.D., and W.P.H. performed the experiments; V.L.K., J.N.B., N.P., S.J.D., and W.P.H. analyzed the data; V.L.K., J.N.B., and H.R.G. interpreted the results of the experiments; V.L.K. and J.N.B. prepared the figures; V.L.K., J.N.B., and H.R.G. drafted the manuscript; V.L.K., J.N.B., P.J.A.K., and H.R.G. edited and revised the manuscript; V.L.K., J.N.B., N.P., S.J.D., W.P.H., P.J.A.K., and H.R.G. approved the final version of the manuscript.

REFERENCES

1. **Albrecht SC, Barata AG, Grosshans J, Teleman AA, Dick TP.** In vivo mapping of hydrogen peroxide and oxidized glutathione reveals chemical and regional specificity of redox homeostasis. *Cell Metab* 14: 819–829, 2011.
2. **Amini A, Masoumi-Moghaddam S, Ehteda A, Morris DL.** Bromelain and *N*-acetylcysteine inhibit proliferation and survival of gastrointestinal cancer cells in vitro: significance of combination therapy. *J Exp Clin Cancer Res* 33: 92, 2014.
3. **Aon MA, Cortassa S, Maack C, O'Rourke B.** Sequential opening of mitochondrial ion channels as a function of glutathione redox thiol status. *J Biol Chem* 282: 21889–21900, 2007.
4. **Atkuri KR, Mantovani JJ, Herzenberg LA, Herzenberg LA.** *N*-acetylcysteine—a safe antidote for cysteine/glutathione deficiency. *Curr Opin Pharmacol* 7: 355–359, 2007.
5. **Beaudoin JN, Kolossov VL, Hanafin W, DiLiberto S, Kenis PG, Gaskins HR.** Thiol-based antioxidants trigger transient mitochondrial oxidation (Abstract). *FASEB J* 27: 1011. 14, 2013.
6. **Billis P, Will Y, Nadanaciva S.** High-content imaging assays for identifying compounds that generate superoxide and impair mitochondrial membrane potential in adherent eukaryotic cells. *Curr Protoc Toxicol* 59: 25.1.1–25.1.14, 2014.
7. **Booty LM, King MS, Thangaratnarajah C, Majd H, James AM, Kunji ER, Murphy MP.** The mitochondrial dicarboxylate and 2-oxoglutarate carriers do not transport glutathione. *FEBS Lett* 589: 621–628, 2015.
8. **Brewer AC, Mustafi SB, Murray TV, Rajasekaran NS, Benjamin IJ.** Reductive stress linked to small HSPs, G6PD, and Nrf2 pathways in heart disease. *Antioxid Redox Signal* 18: 1114–1127, 2013.
9. **Cacciatore I, Cornacchia C, Pinnen F, Mollica A, Di Stefano A.** Prodrug approach for increasing cellular glutathione levels. *Molecules* 15: 1242–1264, 2010.
10. **Circu ML, Rodriguez C, Maloney R, Moyer MP, Aw TY.** Contribution of mitochondrial GSH transport to matrix GSH status and colonic epithelial cell apoptosis. *Free Radic Biol Med* 44: 768–778, 2008.
11. **Dawson TL, Gores GJ, Nieminen AL, Herman B, Lemasters JJ.** Mitochondria as a source of reactive oxygen species during reductive stress in rat hepatocytes. *Am J Physiol Cell Physiol* 264: C961–C967, 1993.
12. **Dikalov S.** Cross talk between mitochondria and NADPH oxidases. *Free Radic Biol Med* 51: 1289–1301, 2011.
13. **Farkas DL, Wei MD, Febbroriello P, Carson JH, Loew LM.** Simultaneous imaging of cell and mitochondrial membrane potentials. *Biophys J* 56: 1053–1069, 1989.
14. **Finn NA, Kemp ML.** Pro-oxidant and antioxidant effects of *N*-acetylcysteine regulate doxorubicin-induced NF-κB activity in leukemic cells. *Mol Biosyst* 8: 650–662, 2012.
15. **Ghyczy M, Boros M.** Electrophilic methyl groups present in the diet ameliorate pathological states induced by reductive and oxidative stress: a hypothesis. *Br J Nutr* 85: 409–414, 2001.

16. **Gutscher M, Pauleau AL, Marty L, Brach T, Wabnitz GH, Samstag Y, Meyer AJ, Dick TP.** Real-time imaging of the intracellular glutathione redox potential. *Nat Met* 5: 553–559, 2008.
17. **Hanson GT, Aggeler R, Oglesbee D, Cannon M, Capaldi RA, Tsien RY, Remington SJ.** Investigating mitochondrial redox potential with redox-sensitive green fluorescent protein indicators. *J Biol Chem* 279: 13044–13053, 2004.
18. **Jones DP, Go YM.** Redox compartmentalization and cellular stress. *Diabetes Obes Metab* 12 *Suppl* 2: 116–125, 2010.
19. **Kehrer JP, Lund LG.** Cellular reducing equivalents and oxidative stress. *Free Radic Biol Med* 17: 65–75, 1994.
20. **Kehrer JP, Smith CV.** Free radicals and reactive oxygen species. In: *Comprehensive Toxicology*, edited by McQueen CA. Madrid, Spain: Elsevier, 2010, p. 278–307.
21. **Khutornenko AA, Roudko VV, Chernyak BV, Vartapetian AB, Chumakov PM, Evstafieva AG.** Pyrimidine biosynthesis links mitochondrial respiration to the p53 pathway. *Proc Natl Acad Sci USA* 107: 12828–12833, 2010.
22. **Kolossov VL, Beaudoin JN, Hanafin WP, DiLiberto SJ, Kenis PJ, Gaskins HR.** Transient light-induced intracellular oxidation revealed by redox biosensor. *Biochem Biophys Res Commun* 439: 517–521, 2013.
23. **Kolossov VL, Hanafin WP, Beaudoin JN, Bica DE, Diliberto SJ, Kenis PJ, Gaskins HR.** Inhibition of glutathione synthesis distinctly alters mitochondrial and cytosolic redox poise. *Exp Biol Med (Maywood)* 239: 394–403, 2014.
24. **Kolossov VL, Spring BQ, Sokolowski A, Conour JE, Clegg RM, Kenis PJ, Gaskins HR.** Engineering redox-sensitive linkers for genetically encoded FRET-based biosensors. *Exp Biol Med (Maywood)* 233: 238–248, 2008.
25. **Lambert AJ, Brand MD.** Superoxide production by NADH:ubiquinone oxidoreductase (complex I) depends on the pH gradient across the mitochondrial inner membrane. *Biochem J* 382: 511–517, 2004.
26. **Lash LH.** Mitochondrial glutathione transport: physiological, pathological and toxicological implications. *Chem Biol Interact* 163: 54–67, 2006.
27. **Lee YJ, Lee DM, Lee CH, Heo SH, Won SY, Im JH, Cho MK, Nam HS, Lee SH.** Suppression of human prostate cancer PC-3 cell growth by *N*-acetylcysteine involves over-expression of Cyr61. *Toxicol In Vitro* 25: 199–205, 2011.
28. **Levy EJ, Anderson ME, Meister A.** Transport of glutathione diethyl ester into human cells. *Proc Natl Acad Sci USA* 90: 9171–9175, 1993.
29. **Lohman JR, Remington SJ.** Development of a family of redox-sensitive green fluorescent protein indicators for use in relatively oxidizing subcellular environments. *Biochemistry* 47: 8678–8688, 2008.
30. **Mari M, Morales A, Colell A, Garcia-Ruiz C, Fernandez-Checa JC.** Mitochondrial glutathione, a key survival antioxidant. *Antioxid Redox Signal* 11: 2685–2700, 2009.
31. **Menon SG, Sarsour EH, Kalen AL, Venkataraman S, Hitchler MJ, Domann FE, Oberley LW, Goswami PC.** Superoxide signaling mediates *N*-acetyl-L-cysteine-induced G_1 arrest: regulatory role of cyclin D1 and manganese superoxide dismutase. *Cancer Res* 67: 6392–6399, 2007.
32. **Meyer AJ, Dick TP.** Fluorescent protein-based redox probes. *Antioxid Redox Signal* 13: 621–650, 2010.
33. **Mezencev R, Wang L, Xu W, Kim B, Sulchek TA, Daneker GW, McDonald JF.** Molecular analysis of the inhibitory effect of *N*-acetyl-L-cysteine on the proliferation and invasiveness of pancreatic cancer cells. *Anticancer Drugs* 24: 504–518, 2013.
34. **Morgan B, Ezerina D, Amoako TN, Riemer J, Seedorf M, Dick TP.** Multiple glutathione disulfide removal pathways mediate cytosolic redox homeostasis. *Nat Chem Biol* 9: 119–125, 2013.
35. **Morgan B, Sobotta MC, Dick TP.** Measuring E_{GSH} and H_2O_2 with roGFP2-based redox probes. *Free Radic Biol Med* 51: 1943–1951, 2011.
36. **Mukhopadhyay P, Rajesh M, Yoshihiro K, Hasko G, Pacher P.** Simple quantitative detection of mitochondrial superoxide production in live cells. *Biochem Biophys Res Commun* 358: 203–208, 2007.
37. **Oyewole AO, Wilmot MC, Fowler M, Birch-Machin MA.** Comparing the effects of mitochondrial targeted and localized antioxidants with cellular antioxidants in human skin cells exposed to UVA and hydrogen peroxide. *FASEB J* 28: 485–494, 2014.
38. **Perry SW, Norman JP, Barbieri J, Brown EB, Gelbard HA.** Mitochondrial membrane potential probes and the proton gradient: a practical usage guide. *Biotechniques* 50: 98–115, 2011.
39. **Qanungo S, Wang M, Nieminen AL.** *N*-acetyl-L-cysteine enhances apoptosis through inhibition of nuclear factor-κB in hypoxic murine embryonic fibroblasts. *J Biol Chem* 279: 50455–50464, 2004.
40. **Raftos JE, Whillier S, Chapman BE, Kuchel PW.** Kinetics of uptake and deacetylation of *N*-acetylcysteine by human erythrocytes. *Int J Biochem Cell Biol* 39: 1698–1706, 2007.
41. **Rajasekaran NS, Connell P, Christians ES, Yan LJ, Taylor RP, Orosz A, Zhang XQ, Stevenson TJ, Peshock RM, Leopold JA, Barry WH, Loscalzo J, Odelberg SJ, Benjamin IJ.** Human α_B-crystallin mutation causes oxido-reductive stress and protein aggregation cardiomyopathy in mice. *Cell* 130: 427–439, 2007.
42. **Sen CK, Packer L.** Thiol homeostasis and supplements in physical exercise. *Am J Clin Nutr* 72: 653S–669S, 2000.
43. **Singh F, Charles AL, Schlagowski AI, Bouitbir J, Bonifacio A, Piquard F, Krahenbuhl S, Geny B, Zoll J.** Reductive stress impairs myoblasts mitochondrial function and triggers mitochondrial hormesis. *Biochim Biophys Acta* 1853: 1574–1585, 2015.
44. **Suski JM, Lebiedzinska M, Bonora M, Pinton P, Duszynski J, Wieckowski MR.** Relation between mitochondrial membrane potential and ROS formation. *Methods Mol Biol* 810: 183–205, 2012.
45. **Taiwo FA.** Mechanism of tiron as scavenger of superoxide ions and free electrons. *Spectroscopy* 22: 491–498, 2008.
46. **Yang J, Su Y, Richmond A.** Antioxidants tiron and *N*-acetyl-L-cysteine differentially mediate apoptosis in melanoma cells via a reactive oxygen species-independent NF-κB pathway. *Free Radic Biol Med* 42: 1369–1380, 2007.
47. **Zafarullah M, Li WQ, Sylvester J, Ahmad M.** Molecular mechanisms of *N*-acetylcysteine actions. *Cell Mol Life Sci* 60: 6–20, 2003.
48. **Zeevalk GD, Manzino L, Sonsalla PK, Bernard LP.** Characterization of intracellular elevation of glutathione (GSH) with glutathione monoethyl ester and GSH in brain and neuronal cultures: relevance to Parkinson's disease. *Exp Neurol* 203: 512–520, 2007.
49. **Zhang F, Lau SS, Monks TJ.** The cytoprotective effect of *N*-acetyl-L-cysteine against ROS-induced cytotoxicity is independent of its ability to enhance glutathione synthesis. *Toxicol Sci* 120: 87–97, 2011.
50. **Zhang H, Limphong P, Pieper J, Liu Q, Rodesch CK, Christians E, Benjamin IJ.** Glutathione-dependent reductive stress triggers mitochondrial oxidation and cytotoxicity. *FASEB J* 26: 1442–1451, 2012.